THE JOURNAL OF PHYSICAL CHEMISTRY B

Article

pubs.acs.org/JPCB

Radiation-Induced Fragmentation of Diamide Extraction Agents in Ionic Liquid Diluents

Ilya A. Shkrob,*[,†] Timothy W. Marin,[†,‡] Jason R. Bell,[§] Huimin Luo,[§] Sheng Dai,[∥] Jasmine L. Hatcher,[⊥] R. Dale Rimmer,[⊥] and James F. Wishart[⊥]

[†]Chemical Sciences and Engineering Division, Argonne National Laboratory, 9700 S. Cass Ave, Argonne, Illinois 60439, United States

[‡]Chemistry Department, Benedictine University, 5700 College Road, Lisle, Illinois 60532, United States

[§]Energy and Transportation Science Division, Oak Ridge National Laboratory, Oak Ridge, Tennessee 37831, United States

[∥]Chemical Sciences Division, Oak Ridge National Laboratory, Oak Ridge, Tennessee 37831, United States

[⊥]Chemistry Department, Brookhaven National Laboratory, Upton, New York 11973-5000, United States

Supporting Information

ABSTRACT: *N,N,N′,N′*-Tetraalkyldiglycolamides are extracting agents that are used for liquid−liquid extraction of trivalent metal ions in wet processing of spent nuclear fuel. This application places such agents in contact with the decaying radionuclides, causing radiolysis of the agent in the organic diluent. Recent research seeks to replace common molecular diluents (such as *n*-dodecane) with hydrophobic room-temperature ionic liquids (ILs), which have superior solvation properties. In alkane diluents, rapid radiolytic deterioration of diglycolamide agents can be inhibited by addition of an aromatic cosolvent that scavenges highly reactive alkane radical cations before these oxidize the extracting agent. Do aromatic ILs exhibit a similar radioprotective effect? To answer this question, we used electron paramagnetic resonance spectroscopy to study the fragmentation pathways in radiolysis of neat diglycolamides, their model compounds, and their solutions in the ILs. Our study indicates that aromatic ILs do not protect these types of solutes from extensive radiolytic damage. Previous research indicated a similar lack of protection for crown ethers, whereas the ILs readily protected di- and trialkyl phosphates (another large class of metal-extracting agents). Our analysis of these unanticipated failures suggests that new types of organic anions are required in order to formulate ILs capable of radioprotection for these classes of solutes. This study is a cautionary tale of the fallacy of analogical thinking when applied to an entirely new and insufficiently understood class of chemical materials.

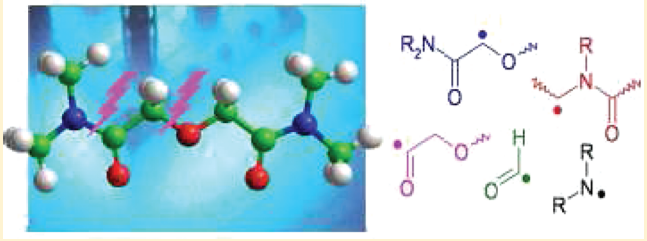

1. INTRODUCTION

Processing of spent nuclear fuel involves chemical separations of U, Pu, Np, minor actinides (Am, Cm), and fission products, such as lanthanides (Ln).[1,2] Some of these products are incorporated in solid matrices for long-term storage, while the remainder can be used to close the nuclear cycle. Trivalent metal ions (such as Ln and minor actinides) can be separated using *N,N,N′,N′*-tetraalkyl-substituted diglycolamides (Scheme 1),[1−5] where the substituting groups can be, for example, *n*-octyl or 2-ethylhexyl. This substitution adds hydrophobicity to the ligand molecule, so that the resulting neutral complex is extracted into a nonpolar organic solvent, such as *n*-dodecane. Another class of such diamide-based extracting agents involves dimalonamides (Scheme 1),[1,6,7] where X is a (long) aliphatic or ether arm and R is a shorter arm. In both cases, the metal ion (M^{3+}) extracted from the nitric acid raffinate is bound through the carbonyl groups of the molecule (L), forming neutral $ML_x(NO_3)_3$ complexes (x = 2−4) in reverse micelles containing water and nitric acid.[2,8] A typical example of such a process is DIAMEX (diamide extraction),[1,2,9] which has been developed as an alternative to the TRUEX (transuranic extraction)[10] process that is based on using a phosphor−organic extracting agent, octyl(phenyl)-*N,N′*-dibutylcarbamoylmethylphosphine oxide in combination with tributylphosphate (that serves both as a coligand and a solvent modifier). The DIAMEX process[5−7,9] was developed to exclude chemicals that cannot be combusted[2] in order to simplify handling and disposal of spent organic

Scheme 1. Chemical Structures for Diamide Extracting Agents Used in Nuclear Separations and the Fragmentation Pathways Observed in Radiolysis

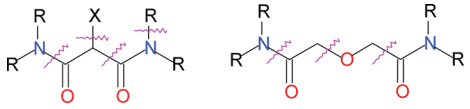

dimalonamides *diglycolamides*

Received: December 6, 2011
Revised: January 17, 2012
Published: February 1, 2012

   dx.doi.org/10.1021/jp2117483 | *J. Phys. Chem. B* 2012, 116, 2234−2243

Scheme 2. A Sketch of Radiation Chemistry of Diglycolamides

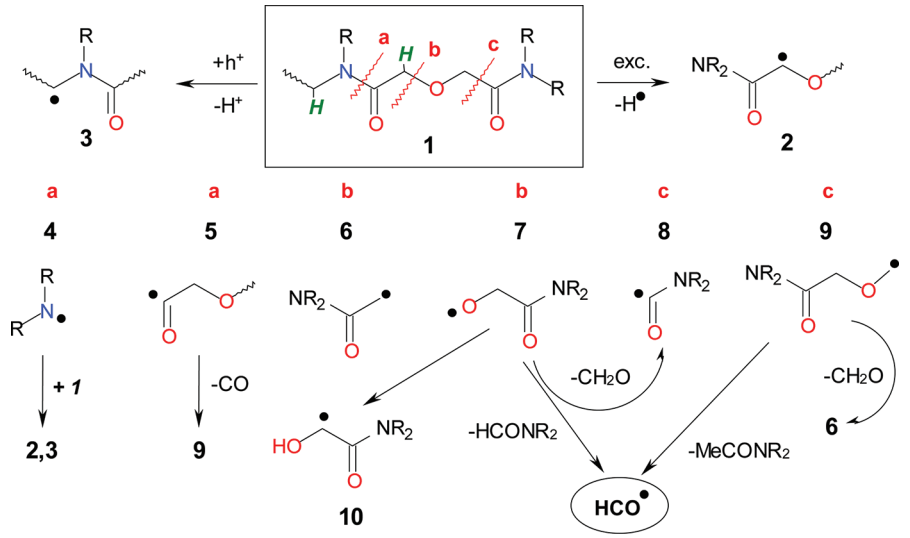

solutions. Dimalonamides[6,7] and *N,N,N′,N′*-tetra(*n*-octyl)diglycolamide (TODGA)[1−5] are commonly used in these processes, and the corresponding monoamides are used as solvent modifiers to improve the solubility of the metal ion complexes in the organic diluent.[1] One of the advantages of the DIAMEX process[9] over TRUEX[10] is improved radiation stability of the extracting agent, at least, under some regimes (see below).[1,2,9] The mono-, di-, and trialkylphosphate esters readily dealkylate upon their exposure to decaying radionuclides,[1,11,12] while the extent of the alkylation in the phosphate has a considerable effect on extraction selectivity.[1]

Recently, there has been growing interest in replacing conventional, molecular organic diluents used in nuclear separations with hydrophobic room temperature ionic liquid (IL) solvents.[13−26] These ILs are salts composed of irregularly shaped cations (such as 1-alkyl-3-methylimidazolium and *N*-alkylpyridinium) and inorganic anions (such as hexafluorophosphate, PF_6^-, and bis(trifluoromethylsulfonyl)amide, NTf_2^-, where Tf = CF_3SO_2).[13] Such ILs have widely tunable physicochemical properties, as the number of ion combinations is astronomical. These ionic liquids combine low volatility, high electric conductivity and polarity, and excellent ion-solvation properties which together make ILs an attractive choice for nuclear separations and open exciting possibilities for conceptually new processes, such as the selective metal ion extraction followed by electrolytic postprocessing.[19] Furthermore, as the diluent consists of ions, heterophase ion exchange can be used instead of neutral extraction.[20−22] There are currently several reports of using diamide-based extracting agents in ILs,[23−26] suggesting the occurrence of the ion-exchange regime at low acidity; further tuning of cation hydrophobicity might be required to avoid such undesirable exchange.[18,21,23]

The problem addressed in the present study deals with a different facet of solvent development: *are diamide extracting agents radiolytically stable in ILs?* To conserve space, some sections, schemes, tables, and figures have been placed in the Supporting Information. Such figures have designator "S" (e.g., Figure 1S).

The current understanding of the radiation chemistry of diamides[1,2,27−30] is based primarily on product analyses that are summarized in Figure 1S;[1,30] this yields the bond-breaking pattern summarized in Schemes 1 and 2. As seen from these schemes, the diamides are polyfunctional molecules that can fragment in multiple ways. The radiolytic decomposition of neat TODGA is very efficient, 8.5 ± 0.9 molecules per 100 eV absorbed, and the decomposition of TODGA in 0.1 M solution in *n*-dodecane in contact with 3 M nitric acid (1:1 v/v) is appreciable, ∼3.7 molecules per 100 eV.[1,30] Generally, ionizing radiation causes the formation of excited states of the molecules (that are frequently dissociative) and also radical ions through the autoionization of these excited states. In organic materials, the resulting radical ions tend to be short-lived, thereby fragmenting to radicals; further reactions of these (neutral) radicals yield the observed reaction products. The fragmentation pathways illustrated in Scheme 2 and Figure 1Sb have been deduced for TODGA in the organic phase in contact with aqueous raffinate, and so it involves both radiolytic damage and hydrolytic cleavage.[1] The radiation stability of TODGA in *n*-dodecane is lowered as compared to neat TODGA,[1,27] as this alkane solvent (due to its high ionization potential) efficiently transfers positive charge to the solute, which results in the formation of the dissociative radical cations.[27,28] Such transfer is apparent from the concave dependence of the *G* value for TODGA decomposition on the mole fraction of the alkane solvent, and it can also be observed directly using pulse radiolysis.[27] This sensitization is reduced by introduction of "hole scavengers", such as aromatic molecules (that react with the alkane radical cations), but the concentration that is necessary to reduce the occurrence of electron transfer from TODGA to the *n*-dodecane$^{\bullet+}$ significantly is very high, 25−50 mol %.[27] Given these observations, we hypothesized that aromatic IL diluents could be superior to molecular solvents like *n*-dodecane because the "holes" (electron deficiencies) and the excess electrons can be trapped by the constituting ions.

While the radiolytic degradation of TODGA is relatively rapid, the deterioration of the *performance* of this extracting agent in Eu(III) and Am(III) extractions under acidic conditions (typical of the forward extraction) is relatively slow.[1,2] The main detrimental effect of TODGA radiolysis is the increase in the retention of trivalent ions under the low acidity conditions that are used for back-extraction due to the interference from 2-(2-(dioctylamino)-2-oxoethoxy)acetic acid that serves as an ion complexant (see Figure 1Sb);[1,30] another concern is the formation of dioctylamine that causes the retention of molybdate in the organic phase during this back-extraction.[2]

dx.doi.org/10.1021/jp2117483 | J. Phys. Chem. B 2012, 116, 2234−2243

Both of these undesirable products are formed through deamination pathway *a* shown in Scheme 2. Thus, one of the main objectives of this study is establishing the reaction mechanisms leading to deamination and assessing the extent of this reaction in IL solutions.

In Scheme 2, we used the fragmentation pattern observed in product analyses to hypothesize on the nature of first-generation radicals derived from a generic diglycolamide (**1**), assuming, hypothetically, that the bond scissions are homolytic. Our previous studies[31] suggested that the corresponding radical cations rapidly deprotonate from the site next to the nitrogen in the aliphatic arm forming radical **3**; for **1**, deprotonation from the methylene protons is also possible, although less likely (section 3.1). Many of these primary radicals are unstable even at low temperature, yielding secondary radicals. Direct observation of these radicals can clarify the mechanisms involved. To this end, we used matrix isolation electron paramagnetic resonance (EPR) spectroscopy to survey the radicals generated in radiolysis of neat diglycolamides and their solutions in ILs.

2. EXPERIMENTAL AND COMPUTATIONAL METHODS

The reagents used in this study have been obtained from Aldrich except for TODGA and *N,N,N′,N′*-tetramethyldiglycolamide (TMDGA) that was substituted either with all methyl (h_{12}) or trideuteromethyl (d_{12}) groups. The latter two compounds were used as a model for TODGA; TMDGA is also used as a masking agent for ions of f-elements in aqueous raffinate.[2] The synthesis of these compounds is discussed in section 1S, and the ^{1}H NMR spectra are given by Figures 2S and 3S in the Supporting Information.

The synthesis of perdeuterated *N*-ethylpyridinium bis(trifluoromethylsulfonyl)amide (EtPy NTf_2) is also given therein. The ionic liquid used as the solvent for the pulse radiolysis kinetics experiments, *N*-methyl-*N*-butylpyrrolidinium bis(trifluoromethylsulfonyl)amide (C_4mpyrr NTf_2), was purchased from IoLiTec USA (Tuscaloosa, AL) and used as supplied after being tested for sufficient purity as described below.

Spectroscopic and computational approaches used in this study were similar to those used in the companion study of the monoamides.[31] The samples were frozen by rapid immersion in liquid nitrogen and irradiated to 1−3 kGy (1 Gy = 1 J/kg) at 77 K using 3 MeV electrons. The radicals were observed using a 9.44 GHz Bruker ESP300E spectrometer, with the sample placed in a flow He cryostat (Oxford Instruments CF935). The magnetic field and the hyperfine coupling constants (hfcc) are given in the units of gauss (1 G = 10^{-4} T). If not stated otherwise, the first-derivative EPR spectra were obtained at 50 K using 2 G modulation at 100 kHz. Where it was possible, the radiation-induced EPR signal from the E'_γ center in the Suprasil sample tubes was deleted from the EPR spectra. The narrow resonance lines from $H^\bullet$ atoms in the glass tubes were also deleted from EPR spectra. To observe radicals originating from redox reactions, aqueous (0.25 M) solutions of TMDGA were mixed with a pH = 2 solution of 2 nm anatase nanoparticles,[32] the solutions were frozen and then irradiated using 40 mJ, 6 ns pulses of 355 nm light from a Nd:YAG laser (Figure 1a). Such spectra exhibit resonance lines from Ti^{3+} ions that were excluded from the plots shown in Figure 1a.

Pulse radiolysis transient absorption kinetics measurements to investigate the reactivity of TMDGA with solvated electrons in C_4mpyrr NTf_2 were carried out at the Brookhaven's LEAF picosecond pulse radiolysis facility.[33] Before radiolysis kinetics studies were performed using a given batch of C_4mpyrr NTf_2,

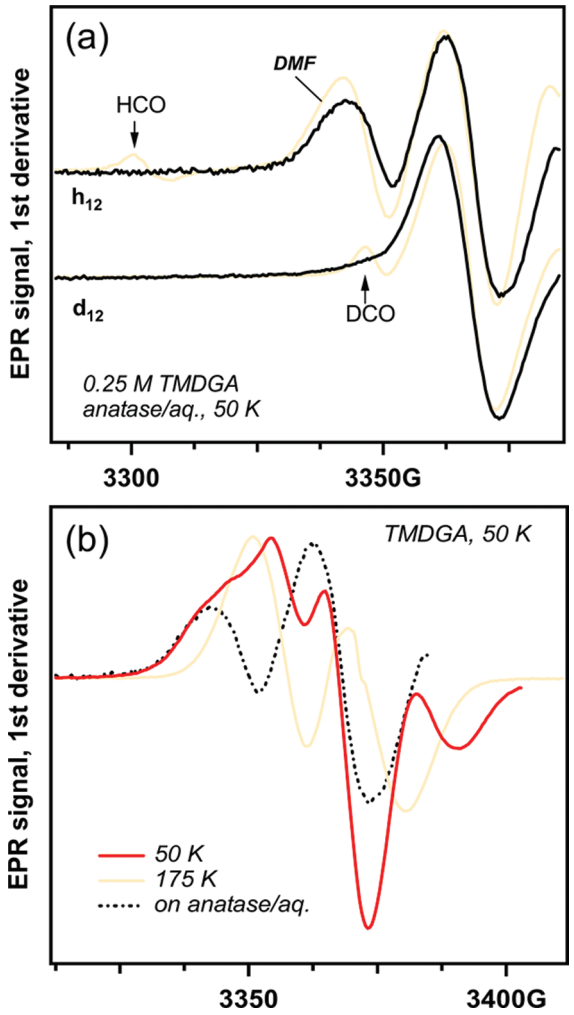

Figure 1. (a) First-derivative EPR spectra (solid lines) of frozen aqueous solutions of 0.25 M TMDGA-h_{12} and -d_{12} containing anatase nanoparticles and irradiated by 355 nm laser light at 77 K. These EPR spectra were obtained using a microwave power of 2 mW at 50 K. For comparison, spectra for DMF-h_7 and DMF-d_7 are shown in the same plot. The low-field resonance lines of the formyl and deuteroformyl radicals are indicated with arrows. (b) EPR spectra of TMDGA-h_7 obtained by irradiation of the quenched melt by 3 MeV electrons at 77 K. These EPR spectra are obtained at 50 and 175 K (see the legend in the plot). For comparison, the EPR spectrum (mainly, from radical **3**) from the aqueous anatase solution of TMDGA-h_{12} from (a) is superimposed onto these two EPR spectra.

the lifetime of the solvated electron in Ar-purged C_4mpyrr NTf_2 was measured by transient absorption at 900 nm. If the electron lifetime was on the order of 1 μs or longer, the batch of IL was deemed sufficiently free of adventitious scavengers to be used for kinetics measurements.[34] In order to obtain the rate constant for the reaction of solvated electrons with TMDGA, solutions of 0, 65, 115, 203, and 247 mM TMDGA in C_4mpyrr NTf_2 were prepared in 1 cm Suprasil self-masking semi-micro spectrophotometer cuvettes capped with silicone septa and purged with argon. The experimental data collection system were described in a previous publication.[33]

The calculations of the hyperfine coupling constants (hfcc) and the optimized structures for the radicals were carried out using a density functional theory (DFT) method with the B3LYP functional[35] and 6-31+G(d,p) basis set from Gaussian 98.[36] In the following, *a* denotes the isotropic hfcc and

dx.doi.org/10.1021/jp2117483 | J. Phys. Chem. B 2012, 116, 2234−2243

B denotes the principal values of **B**, which is the anisotropic part of the hfc tensor **A**. The isotropic hfcc's for various radicals discussed (calculated and reported from the literature) are summarized in Table 1S. Simulations of EPR spectra involved angle averaging using first-order perturbation theory. We point out that since the deuteron (spin 1) has a smaller magnetic moment than the proton (spin 1/2), the hfcc's for the former are 15.3% of the latter, which causes the "collapse" of the resonance lines (reducing the spacing between them). We used such H/D substitution for analysis of congested EPR spectra, as shown below.

3. RESULTS

3.1. Photooxidation of Aqueous TMDGA. Figure 1 exhibits EPR spectra of TMDGA-h_{12} and -d_{12} on aqueous anatase particles photoirradiated by 355 nm light, with EPR spectra from 1 M *N,N*-dimethylformamide, DMF (h_7 and d_7 isotopomers, respectively), obtained under the same conditions. The latter EPR spectra exhibit low-field lines from the formyl (HC$^{\bullet}$O) and deuterioformyl (DC$^{\bullet}$O) radicals generated via photocatalytic reduction of DMF.[31] The triplet of resonance lines from $^{\bullet}CH_2(CH_3)NCHO$ and the singlet from $^{\bullet}CD_2(CD_3)NCHO$ (these identifications are justified in ref 31) originate through the oxidation of DMF by $Ti^{4+}-O^{\bullet}$ radicals photogenerated on the anatase surface. As seen from this plot, EPR spectra for DMF and TMDGA are very similar, suggesting that the photooxidation of TMDGA yields mainly radical **3** shown in Scheme 2.

To demonstrate this point, in Figure 4S we simulated EPR spectra for all (perprotio) radicals shown in Scheme 2, using our DFT estimates for their hfcc's and assuming spherically symmetrical **g** tensors. As seen from Figure 4S, the corresponding EPR spectra fall into three categories: the singlet line for acyl radical **5**, the doublets for ⟩C$^{\bullet}$H radicals **2** and **10** (which cannot be readily distinguished spectroscopically), and the (nearly) spectrally indistinguishable triplets from all other radicals. The photooxidation can result (in principle) in either radical **2** or **3**. Had radicals **2** been generated on anatase as a minority product, their doublet would be masked by the stronger triplet from **3**-h_{11}. However, upon H/D substitution in the methyl groups, this triplet collapses to a singlet line, whereas the EPR spectrum of radical **2**-h_{12} remains the same, as the methyl protons are not coupled to the unpaired electron on the methylene carbon (Table 1S). Therefore, the doublet of radical **2** would still be observed. The absence of this doublet in the EPR spectrum obtained for TMDGA-d_{12} suggests that *the H atom loss via photooxidation involves exclusively methyl protons of TMDGA*.

3.2. Irradiation of Neat Diamides. Figure 1b exhibits the EPR spectrum obtained at 50 and 175 K by 3 MeV electron irradiation of TMDGA-h_{12} rapidly quenched from a melt at 77 K. EPR spectra observed at intermediate temperatures are shown in Figure 5S(a). The well-resolved doublet that is observed above 125 K is certainly from the ⟩C$^{\bullet}$H radicals, so radiolysis of TMDGA, unlike photooxidation examined in section 3.1 does result in H atom loss from the methylene site (Scheme 2). This observation argues against the origin of such radicals from the ground state parent radical cations. In Figure 1b, the EPR spectrum of irradiated TMDGA is superimposed on the EPR spectrum of radical **3** from Figure 1a. It is seen that this radical contributes to the overall EPR spectrum, but the predominant feature in this EPR spectrum is the highly anisotropic singlet line corresponding to a radical with principal components of the **g** tensor of {2.0095, 2.0034, 2.0001}. We attribute this resonance line to the acyl radical **5** since it is uncoupled to the protons and has an anisotropy typical for this type of radicals (e.g., for the $CH_3C^{\bullet}O$ **g** = {2.0038, 2.0022. 1.960}).[37]

Figure 2a shows an EPR spectrum of the same irradiated sample obtained using a wider field range. The resonance lines

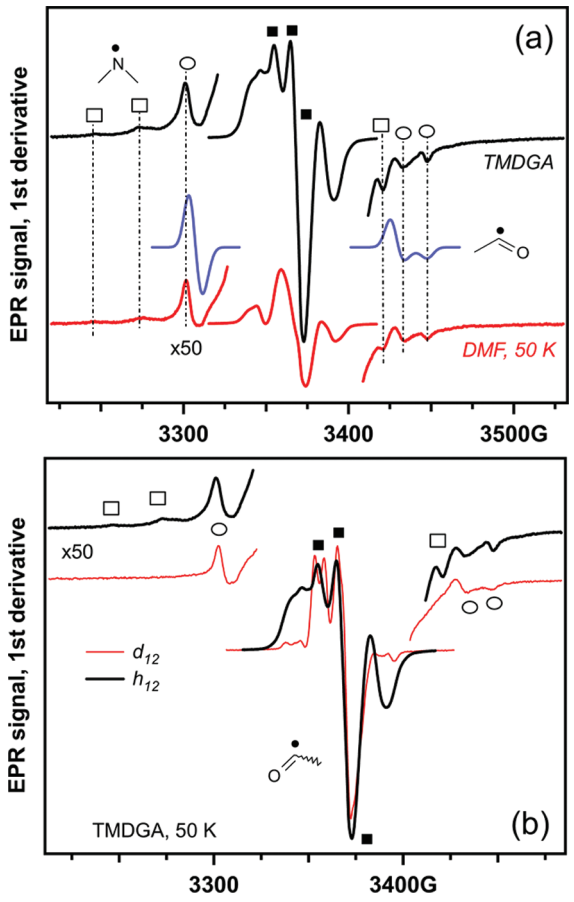

Figure 2. (a) EPR spectra from irradiated TMDGA-h_{12} (quenched melt) compared to DMF-h_7. Superimposed on these EPR spectra is the simulated EPR spectrum of the formyl radical (indicated with open circles). The lines from radical **4** (Scheme 2) are indicated with open squares, and the resonance lines from radical **5** are indicated with filled squares. (b) Comparing EPR spectra from TMDGA-h_{12} and TMDGA-d_{12}.

observed in the spectral wings are very similar to those observed for DMF-h_7 in ref 31 and attributed therein to the formyl and dimethylamidogen (**4**) radicals. The latter decays after warming of the sample to 75 K, whereas the formyl radical persists to 100 K (Figure 5S(b)). While the C−N scission in DMF can, in principle, account for the formation of the formyl radical and radical **4**, the formation of the formyl radical in TMDGA obviously cannot be explained in the same way. This suggests that the formyl radical is a secondary radical originating through fragmentation pathways *b* and *c* (Scheme 2) by elimination from unstable radicals **7** and/or **9**.

In Figure 2b, we compare EPR spectra for TMDGA-h_{12} and -d_{12}. As may be expected, the formyl radical is still observed (as the proton in HC$^{\bullet}$O originates from the methylene protons, see Scheme 2), whereas radical **4** is no longer a nonet (due to the large hfcc's on the methyl protons, see Table 1S) being transformed into a broad, unresolved triplet (due to the anisotropic hyperfine coupling to ^{14}N).[31] The EPR spectrum of the acyl radical **5** does not change, but the outer lines of radicals **2** and **3** are not observed as these spectra "collapse" to an unresolved

dx.doi.org/10.1021/jp2117483 | J. Phys. Chem. B 2012, 116, 2234−2243

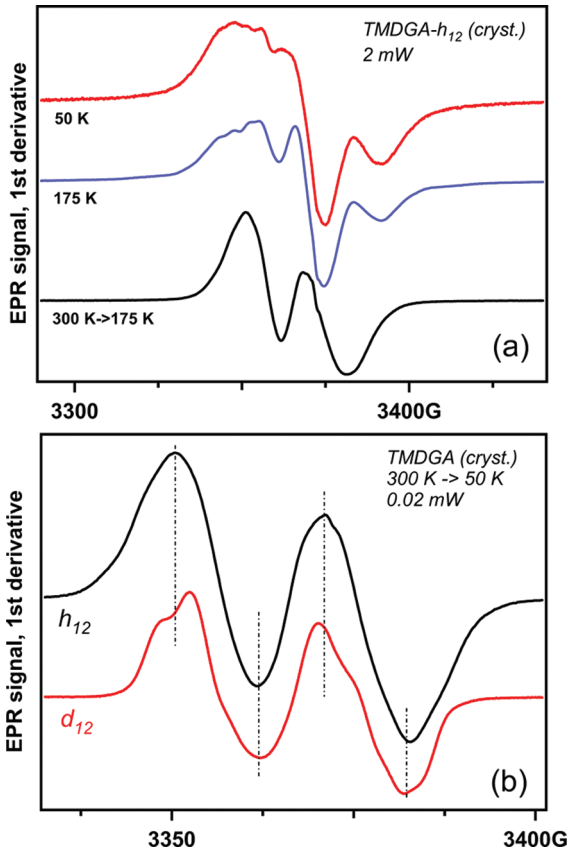

Figure 3. (a) EPR spectra from polycrystalline TMDGA-h_{12} irradiated at 77 K. These EPR spectra were obtained at 50 and 175 K (2 mW); the bottom trace is from a sample that was warmed to the room temperature and subsequently cooled back to 50 K. This trace can be compared with the 175 K trace in Figure 1b (for quenched melt). (b) Comparison of the latter spectrum to the EPR spectrum from polycrystalline TMDGA-d_{12} obtained under the same conditions.

singlet line. Some residual resonance lines are still observed, which can be from radicals **6**, **8**, or **9** postulated in Scheme 2.

To obtain further insight, we irradiated polycrystalline TMDGA (Figure 3), as the crystalline lattice often stabilizes different radicals from the amorphous solid. As shown in Figure 3a, the EPR spectrum from TMDGA-h_{12} observed in the crystals is less resolved, but it has the same components as the EPR spectra shown in Figures 1b and 2. Warming of this crystalline sample to 175 K resolves EPR spectrum and warming to 300 K destroys all radicals except for the $\rangle C^{\bullet}H$ radical. The comparison of EPR spectra for the two isotopomers of this radical in Figure 3b reveals that protonation only broadens the envelope of the lines. These features are expected for radicals **2** and **10**.

Figure 6S(a) exhibits a wide-sweep EPR spectrum for crystalline TMDGA-d_{12}. A more careful examination of the side resonances (that are also seen in Figure 2b) indicates weaker lines (marked with arrows) whose positions coincide with those for the $DC^{\bullet}O$ radical or, alternatively, the outer lines of radical **8**-d_6. These lines are observed only in crystalline TMDGA-d_{12}, but not in the melt. The formation of the deuterioformyl radical is excluded, as the EPR signals from the tentative isotopomers of the formyl behave differently upon warming, and this strongly suggests that these features are from radical **8**. The low yield of this radical implies that fragmentation pathway *c* in Scheme 2 is a minor reaction channel. Examination of the temperature evolution of the "split" doublet seen in Figure 6S(b) and Figure 4a indicates that these resonance lines belong to a single radical. With radicals **8** and **9** excluded, these features can

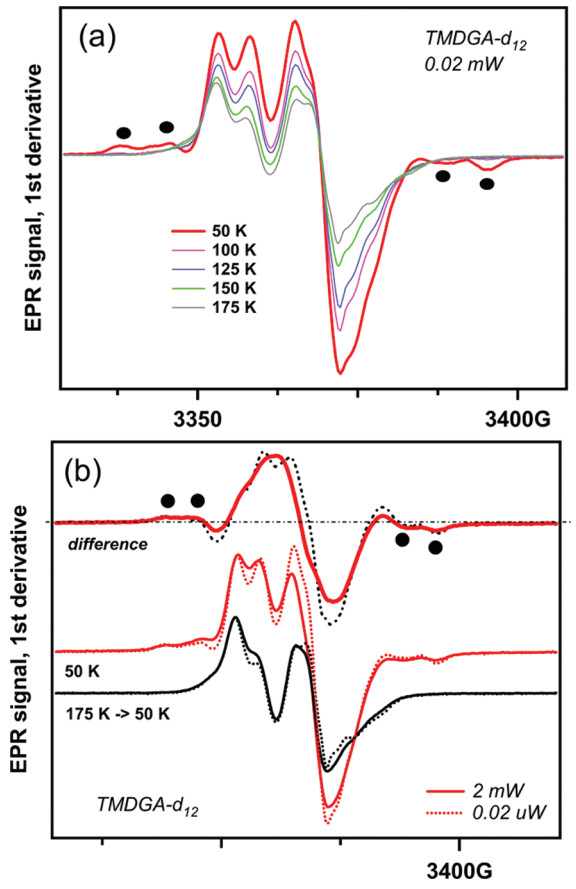

Figure 4. (a) Thermal evolution of EPR spectra from irradiated TMDGA-d_{12} (quenched melt, 0.02 mW). The resonance lines indicated with filled circles are from a radical that decays above 80 K. (b) EPR spectra from the same sample obtained immediately after radiolysis at 77 K (recorded at 50 K) and after warming of this sample to 175 K (both sets were recorded at 2 and 0.02 mW). At the top, the corresponding difference traces are shown. The resonance lines from radical **5** have been subtracted out in this way, as this radical persists to 200 K.

only be from radical **6**, and the "split" in these lines originates through magnetic nonequivalence of the two $^{\bullet}CH_2$ protons. In Figure 4b, we isolated these lines by subtracting EPR spectra obtained from quenched-melt TMDGA-d_{12} observed at 50 K and the same sample warmed to 175 K and subsequently cooled to 50 K. The underlying radicals **2** and **5** persist on warming, and the difference EPR spectrum reveals the lines of the unstable radicals. As seen in Figure 4b, most of the central singlet is from the "collapsed" radical **3**-d_{11}, but it is seen that the "split" lines of radical **6** are indeed the components of a triplet, as we suggested above.

With these insights in mind, we turn to the EPR spectrum for irradiated frozen TODGA shown in Figure 5a, with the EPR spectrum from TMDGA-h_{12} placed alongside for reference. There are several striking differences between these two EPR spectra. First, the yield of the formyl radical in TODGA is so reduced that it cannot be observed. Second, there are several groups of resonance lines (indicated with open circles in the plot) that are certainly from the alkyl radicals (H atom loss radicals from the octyl arms); since all such radicals have similar

dx.doi.org/10.1021/jp2117483 | J. Phys. Chem. B 2012, 116, 2234–2243

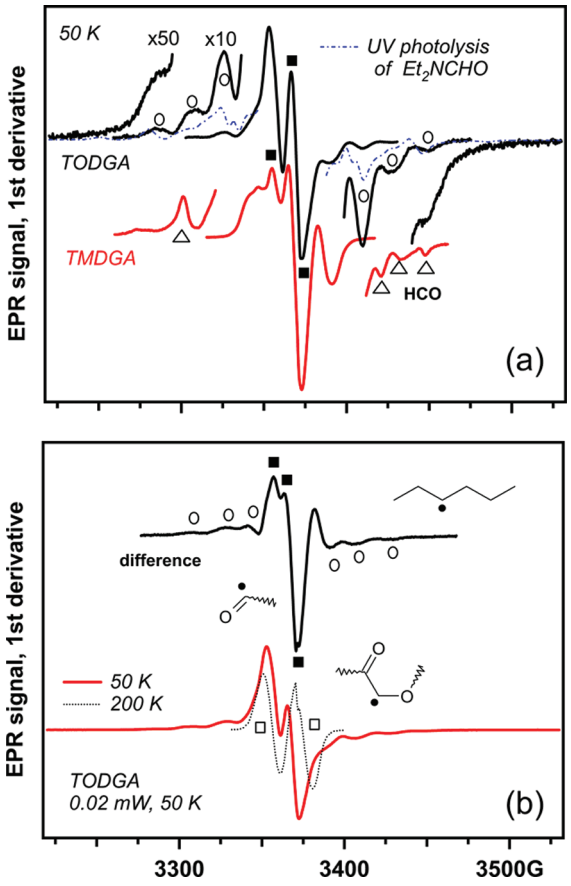

Figure 5. (a) EPR spectra of frozen TODGA and quenched-melt TMDGA-h_{12} irradiated at 77 K and observed at 50 K (0.02 mW). The lines of radical **5** are indicated by filled squares, the lines from the formyl radical are indicated with open triangles, and the lines from the alkyl radical in the octyl arms of TODGA are indicated by open circles. Superimposed on this trace is the EPR spectrum (dash-dot line) of frozen neat *N,N′*-diethylformamide irradiated by 200−300 nm light at 77 K. This EPR spectrum arises mainly from the $Et_2N^{\bullet}$ radical, and it should be similar to that of radical **4** for TODGA. Because of the strong spectral overlap with alkyl radicals, this radical cannot be observed in irradiated TODGA as readily as the $Me_2N^{\bullet}$ can be observed in irradiated TMDGA. (b) EPR spectra from irradiated TODGA obtained at 50 K (solid line) and 200 K (dashed line). The doublet from radical **2** is indicated with open squares. The difference trace reveals the resonance lines from radical **5** without interference from other radical species.

EPR spectra, we cannot identify their precise structure. Third, it is seen that the yield of radical **2** remains significant, despite the fact that the molecule has many more deprotonation sites in the octyl arms than in the methylene groups. This is yet another reason to believe that radical **2** does not originate through the fragmentation of the radical cation of **1**. In Figure 5b, EPR spectra obtained at 50 and 200 K are shown together (a more complete set of EPR spectra obtained at different temperatures is given in Figure 7S). For TODGA, like for TMDGA, warming of the sample eliminates all radicals other than radical **2**. Subtracting these two traces from each other yields the familiar EPR spectrum of radical **5**. Because of the strong overlap with the signals from the alkyl radicals, the presence of radical **4** cannot be verified, as explained in the caption to Figure 5a.

Fragmentation in radiolysis frequently follows the same pattern as ion fragmentation in the gas phase. To examine the latter, we obtained electrospray ionization tandem mass spectra by collisional activation of $M + 1$ cations (protonated molecules) for TMDGA and TODGA (Figure 8S). The two strongest mass peaks for TMDGA correspond to the elimination of dimethylamine (∼90%, pathway *a*, Scheme 2) and DMF (∼10%, pathway *c*); for TODGA these two channels are more even. The prevalence of pathway *a* over *b* and *c* was also suggested by our EPR results.

3.3. Irradiation of TMDGA in Ionic Liquids. Radiolysis of ionic liquids yields many types of radicals, and the resulting EPR spectra are very congested. To recognize EPR lines from radicals derived from TMDGA, high concentration of the solute is required, which greatly exceeds the concentration of the extracting agents (0.1−0.2 M) in a realistic setting.[1,2,9] However, we bear in mind that our goal is not to reproduce working conditions, but rather to address the fundamental and important issue of radioprotection.

Figure 6a exhibits the changes observed in EPR spectra from irradiated solutions of 1-pentyl-3-methylimidazolium

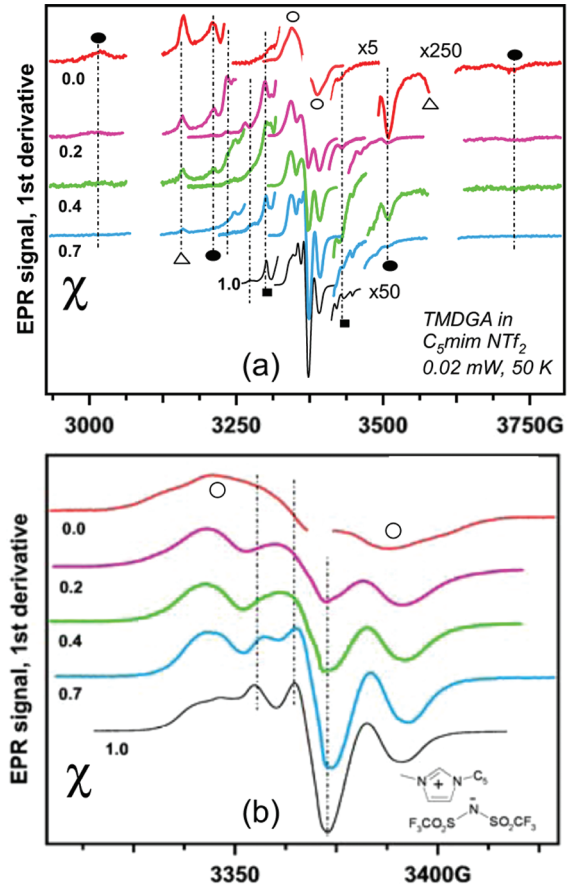

Figure 6. (a) Normalized EPR spectra of frozen solutions of C_5mim NTf_2 (see the structure given in the inset at the bottom) containing TMDGA-h_{12} and irradiated at 77 K. The mole fraction χ of the solute is given in the plot. The doublet indicated with open circles is from the reduced C_5mim^+ cation, the lines of the formyl are indicated with filled squares, and the lines of the $^{\bullet}CF_3$ and $^{\bullet}CF_2SO_2NTf^-$ radicals are indicated with filled circles and open triangles, respectively. (b) The central sections of the EPR spectra are shown in panel b. The resonance lines of radical **5** are indicated with vertical dash-dot lines.

bis(trifluoromethylsulfonyl)amide, C_5mim NTf_2 (see the structural formula in panel b) that contain 0, 20, 40, and 70 mol % of TMDGA-h_{12}. This IL has been chosen for examination due to the high solubility of TMDGA in this solvent. Irradiation of this

dx.doi.org/10.1021/jp2117483 | J. Phys. Chem. B 2012, 116, 2234−2243

imidazolium IL yields a reduced cation (in this particular IL, a dimer radical cation),[38−41] an H atom loss radical in the long arm,[38] and $^{\bullet}CF_3$ and $^{\bullet}CF_2SO_2NTf^-$.[41] Because of the large coupling constants on the ^{19}F nuclei, the latter two radicals have relatively small overlap with the central features that originate from the organic radicals (Figure 6b). Addition of TMDGA-h_{12} to the mixture causes the appearance of the same EPR features that were observed in radiolysis of neat TMDGA-h_{12}, those being the formyl radical and radical **5**. At higher concentration of the solute, radical **2** can also be seen. Warming of these samples above 150 K (Figure 7a) reveals the underlying doublet from radical **2**.

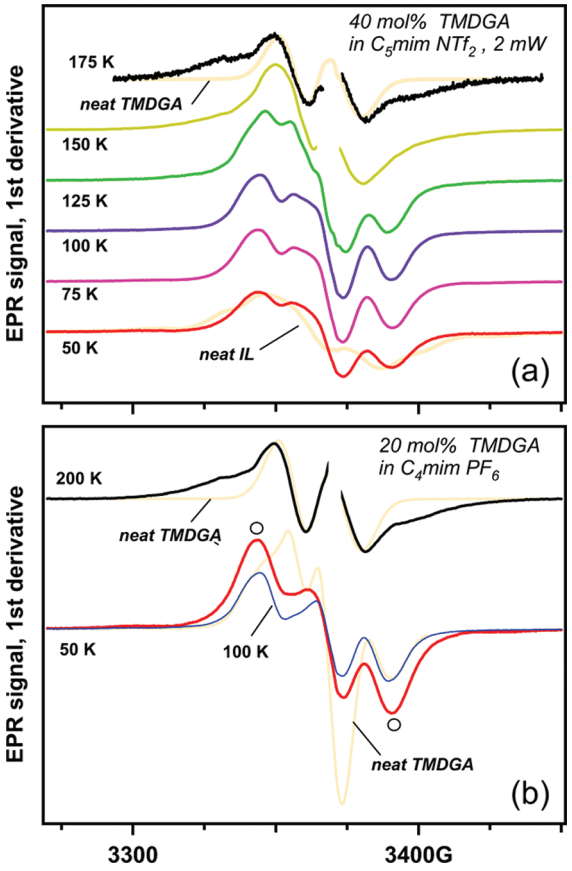

Figure 7. (a) Thermal evolution of EPR spectra (solid lines) of irradiated frozen solution of C_5mim NTf_2 containing 40 mol % TMDGA-h_{12} (2 mW). The temperatures are given in the plot. For comparison, the EPR spectrum of neat irradiated C_5mim NTf_2 (obtained at 50 K) is superimposed on the 50 K trace and the EPR spectrum of neat (quenched-melt) irradiated TMDGA-h_{12} (obtained at 175 K) is superimposed on the 175 K trace. It is seen that radical **2** is present in both of these systems. (b) Radical **2** is also observed in irradiated frozen C_4mim PF_6 containing 20 mol % TMDGA-h_{12}. The lower traces are EPR spectra obtained at 50 and 100 K; the resonance lines indicated with open circles are from the 2-imidazolyl radical generated by the reduction of C_4mim^+ cations. Superimposed on these spectra is the EPR spectrum from neat TMDGA-h_{12}. At the top, the solid black line is the EPR spectrum of the solution obtained at 200 K; superimposed on this trace is EPR spectrum of neat TMDGA-h_{12} obtained at 175 K.

Similar results were obtained for radiolysis of 1-butyl-3-methylimidazolium hexafluorophosphate (C_4mim PF_6) containing 20 mol % TMDGA-h_{12}. In this IL, no anion-derived radicals are observed, and the reduced cation stabilizes as the 2-imidazolyl radical.[38] The EPR spectrum of this radical is a doublet,[38,40] as the unpaired electron on a trigonal carbon-2 is coupled to 2-H in the imidazole ring; there are also weak resonance lines in the wings from the H atom loss radical in the butyl arm (Figure 9S). In the presence of TMDGA-h_{12}, there is a clear line from radical **5** superimposed on the doublet from the 2-imidazolyl (Figure 7b); at 200 K, these EPR signals disappear, and the "hidden" doublet of radical **2** appears. Interestingly, no formyl radical is observed in this system (Figure 9S), suggesting the complete suppression of pathway *b* (Scheme 2).

To observe EPR features from TMDGA with less interference from the ionic liquid matrix, we synthesized an IL containing a perdeuterated cation: *N*-ethylpyridinium-d_{10} bis(trifluoromethylsulfonyl)amide, EtPy-d_{10} NTf_2 (Section 1S). Figure 10S exhibits EPR spectra of neat EtPy-d_{10} NTf_2, neat TMDGA-h_{12}, and a 15 mol % solution of TMDGA-h_{12} in this ionic liquid. In the neat IL, there is a poorly resolved EPR signal from the corresponding *N*-ethylpyridyl radical and also a triplet arising from the $^{\bullet}NTf_2$ radical. In the presence of 15 mol % TMDGA-h_{12}, these features are obscured by the strong resonance lines of the radicals from TMDGA (Figure 10S(a)). These features look very similar to those observed in neat TMDGA-h_{12}; in particular, there is a strong signal from radicals **3** and **5**. An EPR spectrum obtained over a wider range (Figure 10S(b)) reveals the lines of the formyl radical and radical **4** (which is obscured by H atom loss radicals from the IL cations in other IL systems).

All of these results indicate that fragmentation of TMDGA in ionic liquid solutions occurs nearly in the same way as in neat TMDGA. *There is no evidence that the aromatic IL solvent suppresses or promotes radiolytic fragmentation of TMDGA.*

3.4. Pulse Radiolysis of TMDGA in C_4mpyrr NTf_2. To assess the reactivity of electrons toward this family of diamide extractants in ionic liquid media, the kinetics of solvated electron decay (observed at 900 nm, where the solvated electron has an absorption band) in an aliphatic ionic liquid, C_4mpyrr NTf_2, were obtained as a function of TMDGA concentration. The results are shown in Figure 11S(a). Because of the complex behavior of solvated electron decay at low scavenger concentrations, the method of initial rates (first-order kinetic fitting over the range 11−85 ns only) was used to obtain consistent observed rates for determination of the rate constant $(1.08 \pm 0.05) \times 10^8$ M^{-1} s^{-1}; see Figure 11S(b). Notably, this electron scavenging reaction is significantly slower than the common diffusion-controlled limit of $\sim 5 \times 10^8$ M^{-1} s^{-1} for electron reactions with aromatic scavengers in this IL.

Because of the slow relaxation dynamics of ILs, the reactivity of highly mobile, presolvated states of the excess electron are also important.[42,43] The coefficient of presolvated electron scavenging efficiency Q_{37} is defined from $G_c/G_0 = \exp(-cQ_{37})$, where G_c is the yield of solvated electrons at a given scavenger concentration c and G_0 is the yield in the absence of scavenger. Ratios of G_c/G_0 are obtained from initial absorbances calculated by extrapolating the electron decay kinetics to time zero, where Q_{37} is the reciprocal of the concentration C_{37} $(= 1/Q_{37})$ where only $1/e$ (37%) of the electrons survive to be solvated. The larger the Q_{37} (or the smaller the C_{37}), the more efficient the reactant is at scavenging the electrons before they become solvated. The value of Q_{37} obtained from the kinetic traces in Figure 11S is 1.6 ± 0.1 M^{-1} (or $C_{37} = 0.63$ M), which is indicative of TMDGA being a rather poor presolvated electron scavenger.[42−44]

dx.doi.org/10.1021/jp2117483 | J. Phys. Chem. B 2012, 116, 2234−2243

4. DISCUSSION

According to our DFT calculations (section 2), gas-phase (homolytic) bond dissociation energies for (i) methylene C−H and pathways (ii) *a*, (iii) *b*, and (iv) *c* in Scheme 2 are respectively (i) 3.95, (ii) 3.54, (iii) 2.71, and (iv) 3.04 eV; i.e., the most energetically favorable fragmentation pathways are *b* and *c*. On the other hand, the estimated triplet energy of the amides is ∼5 eV.[45] This energy is sufficient for dissociation of *all* chemical bonds in the triplet molecule, and the observed patterns could be determined by other factors than these energetics.

Our results indicate that fragmentation occurs mainly via (i) H atom loss from the aliphatic arms (radical **3**) and bridging methylene groups (radical **2**) and (ii) pathway *a* (radicals **4** and **5**, see Scheme 2) and, to a much lesser extent, pathway *b* (formyl radical and radical **6**). We did not find evidence for the loss of the entire aliphatic arms, which is consistent with product analyses.[1,2,29,30] The yield of radical **8** via fragmentation pathway *c* is very low; in fact, it could be a secondary radical generated by elimination of formaldehyde from the oxyl radical **7** generated via pathway *b*, as shown in Scheme 2. The prominence of pathway *c* observed in previous work[1,30] is likely to be from the synergistic action of radiolysis and hydrolytic cleavage (as the product analyses were performed in diluents contacting nitric acid). The loss of H atoms from the aliphatic arms is expected for deprotonation of radical cations (section 3.1), while H atom loss from the methylene groups cannot be explained by oxidation of the parent molecule. Indeed, this mechanism is incompatible with our observation that mild photooxidation of TMDGA exclusively produced radical **3** (section 3.1). Another argument against the formation of radical **2** via the deprotonation of the parent cation is that the yield of this radical does not decrease significantly for TODGA vs TMDGA, while the former molecule has many more deprotonation sites in the aliphatic arms. Both of these observations suggest that radical **2** originates from a dissociative, excited state of **1**, that is, from the C−H bond dissociation in a (most likely, triplet) state formed by the direct excitation of **1** or via charge recombination. The resulting H atom abstracts hydrogen from the aliphatic arms. Note that the perceived low yield of the resulting alkyl radicals (Figure 5a) vs radical **2** is due to the wider span of the EPR spectrum for these alkyl radicals; actually, there is near parity in the yields of these two radicals.

In contrast, the large disparity between the yields of radicals **4** and **5** (∼1:8, by double integration) excludes their simultaneous formation via homolytic cleavage of the C−N bond in an excited state, as envisaged in Scheme 2. Furthermore, the preference for pathway *a* over pathways *b* and *c* seems to be inconsistent with such dissociation, as in the ground state molecule, the C−N bond is stronger than the other two bonds. In ref 31, we have observed similar disparities between the radical yields in radiolysis of *N,N*-dimethyl- and diethylformamide, suggesting that the fragmentation occurs in radical ions. The direct evidence for fragmentation of the proton adduct of **1** via the loss of dialkylamine and *N,N*-dialkylformamide is provided by mass spectrometry (section 3.2). We suggest that radicals **4** and **5** are generated by fragmentation of the electronically excited radical cation of **1**; these channels compete with deprotonation of this radical cation. We exclude dissociative electron attachment since there is no evidence for its occurrence even for monoamides.[31]

The high yield of radical **5** and its remarkable stability to decarboxylation (Scheme 2) are responsible for the eventual formation of 2-(2-(dioctylamino)-2-oxoethoxy)acetic acid, which interferes with stripping of the metal ions from the organic phase.[1] Our suggestions rationalize the "radioprotective" effect of benzene on the TODGA/*n*-dodecane mixture observed in ref 27, as the benzene serves both as a hole scavenger and an excited state quencher.

Unfortunately, our expectations that aromatic ILs would exert a radioprotective effect similar to benzene cosolvent in the alkane mixtures were not borne out by our experiments. As shown in section 3.3, the formation of radicals **2** to **5** occurs in these aromatic IL solutions as readily as in neat **1**. On the positive side, there is no evidence for efficient charge and energy transfer from the IL solvent to the solute. On the negative side, there is also no evidence that the dissociative states of **1** or its radical cation are quenched and/or scavenged by the solvent, at least in a low-temperature matrix.

Thus, the "radioprotective" effect of ILs that was observed for dialkyl and trialkyl phosphates (another class of extraction agents) examined in refs 39 and 46 does not seem to extend to the diglycolamides. In our previous studies,[39,41,46] this effect was explained by the remarkable electron trapping properties of aromatic ILs: the excess electron generated in the ionization events is rapidly scavenged by cations as neutral radicals; these radicals can be further stabilized by protonation and/or bond formation with the parent cation.[38] Consequently, electron transfer to the organophosphate solute is inefficient and electron attachment of prethermalized "dry" electrons (that yield highly dissociative phosphoranyl radicals)[46] is suppressed. In the case of diglycolamide solutes this efficient preferential electron trapping by the high concentration of aromatic IL cations still happens; rate constants for solvated electron capture in C_4mpyrr NTf_2 are 6.8×10^8 M^{-1} s^{-1} for C_4mim^+ cation[47] and 6.2×10^8 M^{-1} s^{-1} for *N*-butylpyridinium cation,[48] whereas we measured 1.1×10^8 M^{-1} s^{-1} for TMDGA (section 3.4). We emphasize that the typical concentration of TODGA in extraction solvents is 0.1−0.2 M;[2] i.e., only a small fraction (∼0.5−1%) of the electrons are scavenged by the diglycolamide solute in neat C_4mim NTf_2. Furthermore, TMDGA is only weakly reactive with presolvated electrons (Q_{37} = 1.6 M^{-1}) while C_4mim^+ and *N*-butylpyridinium$^+$ are much more efficient (Q_{37} = 18 and 20 M^{-1}, respectively).[47,48] If nonaromatic ILs are used, TMDGA could potentially scavenge solvated electrons.

However, in reality, efficient electron trapping by an IL does little to protect the diglycolamide extractant because electron attachment to diglycolamides evidently does not induce dissociation. Rather, diglycolamides require protection from the formation of dissociative excited states and/or oxidative fragmentation. Apparently, the lifetimes of these dissociative (neutral or charged) states are so short that even the presence of aromatic cations cannot significantly reduce the fragmentation yields.

Another reason for the lack of radioprotection is the fundamental difference between molecular and ionic solvents: retrospectively, it is apparent that our analogical thinking was flawed. In *n*-dodecane, benzene can protect TODGA because it rapidly scavenges radical cations of the alkane solvent;[27] this positive charge stabilizes as a sandwich dimer radical cation of benzene,[27,49] for which accepting an electron from TODGA is energetically prohibitive. In contrast, in aromatic ILs the "holes" tend to localize on *anions*. Alternatively, the "holes" oxidize cations and yield radical dications; the latter rapidly deprotonate, as the nearby anions serve as strong proton

acceptors. While these radical dications are too short-lived to transfer charge to the solute, the oxidized anions are strong oxidizers. This is particularly true about anions that have large electron detachment energies, such as NTf_2^- and PF_6^-.[41] For this reason, the presence of aromatic cations in an IL diluent does not have the same chemical consequences as the presence of aromatic molecules in a molecular diluent. We have previously noted[50] the failure of aromatic ILs to reduce radiolytic degradation of crown ethers (which are common ionophores in nuclear separations involving Cs^+ and Sr^{2+});[20−22] once again, the decomposition of the solute involved dissociative excited states. Generalizing these observations, aromatic ILs can protect solutes against radiation-induced reduction, but such reduction does not cause fragmentation in crown ethers and diglycolamides, which need protection from a different type of deleterious reaction.

This line of reasoning suggests that the minimization of radiation damage to the latter type of solutes requires ILs in which the constituting anions (A^-) have relatively low electron detachment energies (EDE) (see ref 41), so that the corresponding radicals $A^\bullet$ (oxidized anions) cannot mediate oxidation of the solute. As was demonstrated in ref 41, most of such ILs are subject to cumulative radiation damage, as the radicals $A^\bullet$ rapidly fragment. Such IL diluents may indeed protect the solute against oxidation in radiolysis, but the diluents themselves undergo rapid decomposition. While we found some exceptions to this general rule, viz. anions that had both low EDE for A^- and high stability for $A^\bullet$ (such as benzoate and salicylate),[41] these are not suitable for nuclear separations involving strong acid solutions since these anions are conjugate bases of weak acids and thus would become protonated under process conditions,[46,51] causing undesirable exchange of the IL anion. Thus, practically useful IL diluents should consist of anions that are conjugate bases of strong acids. The design of ILs that satisfies such requirements is beyond the scope of this study.

5. CONCLUSION

We identified intermediate radical products generated in radiolysis of *N,N,N′,N′*-tetraalkyldiglycolamides that are used as extraction agents in nuclear separations involving trivalent metal ions.[2] Our results indicate that these molecules fragment through breaking of their C−H, C−N, and C−O bonds. Some of this fragmentation occurs in electronically excited (most likely, triplet) states; there is also fragmentation in their (excited) radical cations. H atom loss radicals and acyl radicals have the highest yield in radiolysis of neat diglycolamides and their solutions in several aromatic ionic liquids. The latter solvents, contrary to our expectations and the precedent for molecular analogs,[27] did not protect the diglycolamides from radiation-induced fragmentation. The latter causes efficient deamination; the corresponding carboxylate, being a strong anionic complexant, and the amine, being a strong neutral complexant for the molybdate, are known to interfere with back extraction of metal ions at low acidity.[1,2]

Our analysis suggests that most common types of ILs cannot be used for radiation protection of solutes that fragment mainly from their (excited) neutral or positively charged states. A new class of IL constituting anions should be used to this end, and so the problem is not insurmountable but requires *synthetic* innovation.

We emphasize that our conclusions concerning the radioprotective properties of IL solvents are preliminary, as these are based on the behavior observed in low-temperature, frozen IL matrices; there is a possibility that thermally activated reactions of secondary radicals generated in radiolysis could induce additional fragmentation that was not observed at low temperature using EPR spectroscopy.

■ ASSOCIATED CONTENT

Supporting Information

List of abbreviations, synthetic procedures, reported and calculated hfcc's for radical species of interest, and Figures 1S−11S with captions. This material is available free of charge via the Internet at http://pubs.acs.org.

■ AUTHOR INFORMATION

Corresponding Author

*Tel: (630) 252-9516; e-mail: shkrob@anl.gov.

Notes

The authors declare no competing financial interest.

■ ACKNOWLEDGMENTS

The work at Argonne, Oak Ridge, and Brookhaven (including use of the LEAF Facility of the BNL Accelerator Center for Energy Research) was supported by the US-DOE Office of Science, Division of Chemical Sciences, Geosciences and Biosciences under Contracts DE-AC02-06CH11357, DE-AC05-0096OR22725, and DE-AC02-98CH10886, respectively. Programmatic support via a DOE SISGR grant "An Integrated Basic Research Program for Advanced Nuclear Energy Separations Systems Based on Ionic Liquids" is gratefully acknowledged.

■ REFERENCES

(1) Berthon, L.; Chabronnel, M.-C. In *Ion Exchange and Solvent Extraction, A Series of Advances*; Moyer, B. A., Ed.; CRC Press: Roca Baton, FL, 2010; Vol. *19*, pp 429−513.

(2) Ansari, S. A.; Pathak, P.; Mohapatra, P. K.; Manchanda, V. K. *Chem. Rev.* **2011**, DOI: 10.1021/cr200002f.

(3) Sasaki, Y.; Sugo, Y.; Suzuki, S.; Tachimori, S. *Solvent Extr. Ion Exch.* **2001**, *19*, 91−103.

(4) Horwitz, E. P.; McAlister, D. R.; Bond, H.; Barrans, R. E. Jr. *Solvent Extr. Ion Exch.* **2005**, *23*, 319−344.

(5) Sasaki, Y.; Sugo, Y.; Kitatsuji, Y.; Kirishima, A.; Kimura, T.; Choppin, G. R. *Anal. Sci.* **2007**, *23*, 727−731. Magnusson, D.; Christiansen, B.; Glatz, J.-P.; Malmbeck, R.; Modolo, G.; Serrano-Purroy, D.; Sorel, C. *Solvent Extr. Ion Exch.* **2009**, *27*, 26−35. Modolo, G.; Asp, H.; Schreinemachers, C.; Vijgen, H. *Solvent Extr. Ion Exch.* **2007**, *25*, 703−721.

(6) Cuillerdier, C.; Musikas, C.; Hoel, P.; Nigond, L.; Vitart, X. *Sep. Sci. Technol.* **1991**, *26*, 1229−1244.

(7) Thiollet, G.; Musikas, C. *Solvent Extr. Ion Exch.* **1989**, *7*, 813−827.

(8) Jensen, M. P.; Yaita, T.; Chiarizia, R. *Langmuir* **2007**, *23*, 4765−4774.

(9) Serrano-Purroy, D.; Baron, P.; Christiansen, B.; Malmbeck, R.; Sorel, C.; Glatz, J.-P. *Radiochim. Acta* **2005**, *93*, 351−355. Malmbeck, R.; Courson, O.; Pagliosa, G.; Romer, K.; Satmark, B.; Glatz, J.-P.; Baron, P. *Radiochim. Acta* **2000**, *88*, 865−871.

(10) Schultz, W. W.; Horwitz, E. P. *Sep. Sci. Technol.* **1988**, *23*, 1191−1210. Horwitz, E. P.; Kalina, D. C.; Diamond, H.; Vandegrift, G. F.; Schultz, W. W. *Solvent Extr. Ion Exch.* **1985**, *3*, 75−109.

(11) Mincher, B. J.; Mezyk, S. P.; Martin, L. R. *J. Phys. Chem. A* **2008**, *112*, 6275−6280. Mincher, B. J.; Modolo, G.; Mezyk, S. P. *Solvent Extr. Ion Exch.* **2009**, *27*, 1−25 and references therein.

(12) Shkrob, I. A.; Marin, T. W. *Chem. Phys. Lett.* **2008**, *465*, 234−237 and references therein.

(13) Hallett, J. P.; Welton, T. *Chem. Rev.* **2011**, *111*, 3508−3576. Welton, T. *Chem. Rev.* **1999**, *99*, 2071−2083. Plechkova, N. V.;

Seddon, K. R. *Chem. Soc. Rev.* **2008**, *37*, 123−150. Smiglak, M.; Metlen, A.; Rogers, R. D. *Acc. Chem. Res.* **2007**, *40*, 1182−1192. Parvulescu, V. I.; Hardacre, C. *Chem. Rev.* **2007**, *107*, 2615−2665. Binnemans, K. *Chem. Rev.* **2007**, *107*, 2592−2614.

(14) Cocalia, V. A.; Gutowski, K. E.; Rogers, R. D. *Coord. Chem. Rev.* **2006**, *250*, 755−764. Cocalia, V. A.; Jensen, M. P.; Holbrey, J. D.; Spear, S. K.; Stepinski, D. C.; Rogers, R. D. *Dalton Trans.* **2005**, 1966−1971. Jensen, M. P.; Neuefeind, J.; Beitz, J. V.; Skanthakumar, S.; Soderholm, L. *J. Am. Chem. Soc.* **2003**, *125*, 15466−15473.

(15) Dietz, M. L.; Dzielawa, J. A.; Jensen, M. P.; Beitz, J. V.; Borkowski, M. In *Ionic Liquids IIIb: Fundamentals, Progress, Challenges and Opportunities: Transformations and Processes*; American Chemical Society: Washington, DC, 2005; Vol. *902*, pp 2−18. Nash, K. L. In *Separations for the Nuclear Fuel Cycle in the 21st Century*; Lumetta, G. J., Nash, K. L., Clark, S. B., Friese, J. I., Eds.; American Chemical Society: Washington, DC, 2006; Vol. *933*, pp 21−40.

(16) Wishart, J. F. *J. Phys. Chem. Lett.* **2010**, *1*, 3225−3231. Wishart, J. F.; Shkrob, I. A. In *Ionic Liquids: From Knowledge to Application*; Rogers, R. D., Plechkova, N. V., Seddon, K. R., Eds.; American Chemical Society: Washington, DC, 2009; pp 119−134.

(17) Sun, X. Q.; Luo, H. M.; Dai, S. *Chem. Rev.* **2012**, DOI: 10.1021/cr200193x.

(18) Billard, I.; Ouadi, A.; Gaillard, C. *Anal. Bional. Chem.* **2011**, *400*, 1555−1566. Ha, S. H.; Menchavez, R. N.; Koo, Y.-M. *Korean J. Chem. Eng.* **2010**, *27*, 1360−1365.

(19) Chen, P. Y.; Hussey, C. L. *Electrochim. Acta* **2004**, *49*, 5125−5138.

(20) Luo, H. M.; Dai, S.; Bonnesen, P. V.; Haverlock, T. J.; Moyer, B. A.; Buchanan, A. C. III *Solvent Extr. Ion Exch.* **2006**, *24*, 19−31. Luo, H. M.; Dai, S.; Bonnesen, P. V. *Anal. Chem.* **2004**, *76*, 2773−2779. Dai, S.; Ju, Y. H.; Barnes, C. E. *J. Chem. Soc., Dalton Trans.* **1999**, 1201−1202. Luo, H. M.; Dai, S.; Bonnesen, P. V.; Buchanan, A. C. III *J. Alloys Compd.* **2006**, *418*, 195−199. Sun, X. Q.; Bell, J. R.; Luo, H. M.; Dai, S. *Dalton Trans.* **2011**, 8019−8023.

(21) Dietz, M. L.; Stepinski, D. C. *Talanta* **2008**, *75*, 598−603. Dietz, M. L. *Sep. Sci. Technol.* **2006**, *41*, 2047−2063. Dietz, M. L.; Stepinski, D. C. *Green Chem.* **2005**, *7*, 747−750. Dietz, M. L.; Dzielawa, J. A.; Laszak, I.; Young, B. A.; Jensen, M. P. *Green Chem.* **2003**, *5*, 682−685. Dietz, M. L.; Dzielawa, J. A. *Chem. Commun.* **2001**, 2124−2125.

(22) Stepinski, D. C.; Vandegrift, G. F. III; Shkrob, I. A.; Wishart, J. F.; Kerr, K.; Dietz, M. L.; Qadah, D. T. D.; Garvey, S. L. *Ind. Eng. Chem. Res.* **2010**, *49*, 5863−5868.

(23) Shimojo, K.; Kurahashi, K.; Naganawa, H. *Dalton Trans.* **2008**, *37*, 5083−5088.

(24) Turanov, A. N.; Karandashev, V. K.; Baulin, V. E. *Solvent Extr. Ion Exch.* **2010**, *28*, 367−387.

(25) Kubota, F.; Shimobori, Y.; Baba, Y.; Koyanagi, Y.; Shimojo, K.; Kamiya, N.; Goto, M. *J. Chem. Eng. Jpn.* **2011**, *44*, 307−312.

(26) Rout, A.; Karmakar, S.; Venkatesan, K. A.; Srinivasan, T. G.; Rao, P. R. V. *Sep. Purif. Technol.* **2011**, *81*, 109−115.

(27) Sugo, Y.; Izumi, Y.; Yoshida, Y.; Nishijima, S.; Sasaki, Y.; Kimura, T.; Sekine, T.; Kudo, H. *Radiat. Phys. Chem.* **2007**, *76*, 794−800.

(28) Sugo, Y.; Taguchi, M.; Sasaki, Y.; Hirota, K.; Kimura, T. *Radiat. Phys. Chem.* **2009**, *78*, 1140−1144.

(29) Sharma, J. N.; Ruhela, R.; Singh, K. K.; Kumar, M.; Janardhanan, C.; Achutan, P. V.; Manohar, S.; Wattal, P. K.; Suri, A. K. *Radiochim. Acta* **2010**, *98*, 485−491.

(30) Sugo, Y.; Sasaki, Y.; Tachimori, S. *Radiochim. Acta* **2002**, *90*, 161−165.

(31) Shkrob, I. A.; Marin, T. W. *J. Phys. Chem. A* **2012**, DOI: 10.1021/jp2115687.

(32) Shkrob, I. A.; Marin, T. W.; Adhikary, A.; Sevilla, M. D. *J. Phys. Chem. C* **2011**, *115*, 3393−3403.

(33) Wishart, J. F.; Cook, A. R.; Miller, J. R. *Rev. Sci. Instrum.* **2004**, *75*, 4359−4366.

(34) Wishart, J. F. Ionic Liquid Radiation Chemistry. In *Ionic Liquids: COILed for Action*; Seddon, K. R., Rogers, R. D., Eds.; Wiley, Ltd.: Chichester, UK, 2012; in press.

(35) Becke, A. D. *Phys. Rev. A* **1988**, *38*, 3098−3100. Lee, C.; Yang, W.; Parr, R. G. *Phys. Rev. B* **1988**, *37*, 785−789.

(36) Frisch, M. J.; Trucks, G. W.; Schlegel, H. B.; Scuseria, G. E.; Robb, M. A.; Cheeseman, J. R.; Zakrzewski, V. G.; Montgomery, J. A., Jr.; Stratmann, R. E.; Burant, J. C.;et al. *Gaussian 98, rev. A.1*; Gaussian, Inc.: Pittsburgh, PA; 1998.

(37) Landolt-Bornstein, New Series, *Magnetic Properties of Free Radicals*; Fischer, H., Ed.; Springer-Verlag: Berlin, 1987.

(38) Shkrob, I. A.; Marin, T. W.; Chemerisov, S. D.; Hatcher, J. L.; Wishart, J. F. *J. Phys. Chem. B* **2011**, *115*, 3889−3902.

(39) Shkrob, I. A.; Chemerisov, S. D.; Wishart, J. F. *J. Phys. Chem. B* **2007**, *111*, 11786−11793.

(40) Shkrob, I. A.; Wishart, J. F. *J. Phys. Chem. B* **2009**, *113*, 5582−5592.

(41) Shkrob, I. A.; Marin, T. W.; Chemerisov, S. D.; Wishart, J. F. *J. Phys. Chem. B* **2011**, *115*, 3872−3888.

(42) Wishart, J. F.; Funston, A. M.; Szreder, T.; Cook, A. R.; Gohdo, M. *Faraday Discuss.* **2012**, *154*, 353−363.

(43) Wishart, J. F.; Neta, P. *J. Phys. Chem. B* **2003**, *107*, 7261−7267.

(44) Lall-Ramnarine, S. I.; Castano, A.; Subramaniam, G.; Thomas, M. F.; Wishart, J. F. *Radiat. Phys. Chem.* **2009**, *78*, 1120−1125.

(45) Staley, R. H.; Harding., L. B.; Goddard, W. A. III; Beauchamp, J. L. *Chem. Phys. Lett.* **1975**, *36*, 589−593.

(46) Shkrob, I. A.; Marin, T. W.; Chemerisov, S. D.; Wishart, J. F. *J. Phys. Chem. B* **2011**, *115*, 10927−10942.

(47) Takahashi, K.; Sato, T.; Katsumura, Y.; Yang, J.; Kondoh, T.; Yoshida, Y.; Katoh, R. *Radiat. Phys. Chem.* **2008**, *77*, 1239−1243.

(48) Lall-Ramnarine, S. I.; Hatcher, J. L.; Thomas, M. F.; Engel, R. R.; Wishart, J. F. *ChemPhysChem* **2012**, in preparation.

(49) Bradforth, S. E.; Pieniazek, P. A.; Krylov, A. I.; Bradforth, S. E. *J. Chem. Phys.* **2007**, *127*, 044317 and references therein.

(50) Shkrob, I. A.; Marin, T. W.; Dietz, M. L. *J. Phys. Chem. B* **2011**, *115*, 3903−3911.

(51) Marin, T. W.; Shkrob, I. A.; Dietz, M. L. *J. Phys. Chem. B* **2011**, *115*, 3912−3918.